

## **Effects of Pyridine and Furan Pretreatment on the Corrosion Resistance of Rust Coating on Mild Steel**

*Yinze Zuo, Liang Chen, Yu Wang, Yunxia Guo, Xingling Shi\*, Yanmin Gao\**

School of Materials Science and Engineering, Jiangsu University of Science and Technology, Zhenjiang 212003

\*E-mail: sxl\_just@163.com, ymgjust@126.com

*Received: 16 May 2017 / Accepted: 12 July 2017 / Published: 12 September 2017*

---

Pre-processing of a metal surface before coating is a key factor that affects the coating performance. This phenomenon has been puzzling people for a long time. In this paper, a new type of preprocessing using heterocyclic compounds, pyridine and furan, were applied to address this problem. The tests show that the rust layers of mild steel treated by pyridine and furan are more compact than the untreated layers. The corrosion rate of the mild steel with a rust layer treated by pyridine is lower than that of the samples with furan treatment and without treatment, while the impedance is also the largest. The adhesion of an epoxy-polyvinylbutyral (EP-PVB) coating, which is painted on rust layers with pyridine and furan pretreatment, is much stronger. Moreover, the corrosion resistance of EP-PVB coatings that are painted onto the rust layers with pretreatment is much better than that of the coatings that are directly painted onto the rust layer without pretreatment. The impedance of EP-PVB coatings that are painted onto the rust layers with pretreatment is much higher than that of the EP-PVB coating that is directly painted onto the rust layer without pretreatment.

---

**Keywords:** corrosion, surface treatment, rust coating, heterocyclic compounds, electrochemical test

### **1. INTRODUCTION**

For a long time, the corrosion of mild steel has been a considerable problem. Currently, the most ordinary and effective method to protect mild steel is to paint a coating on the metal surface. However, there are various factors that affect the performance of the coating. For instance, surface pretreatment before coating is crucial because rust on the metal surface is detrimental for the coating and shortens the service life of the coating. Although the traditional processing methods, such as blasting and pickling, show many benefits for coating performance, there are many drawbacks as well. Therefore, we must find a new process to handle the rust layer on the metal surface.

Self-assembly is essentially a reaction of two or more molecules via chemical bonds without the interference of external factors[1-3]. Recently, rust coatings have received considerable attention from researchers as self-assembly technology has been gradually applied [4-10]. The unique feature of a rust coating is that it contains a certain amount of rust converters. The rust converters can transform loose rust into a harmless filler in the coating. The formation of self-assembled monolayers (SAMs) is a spontaneous chemical process. It has strong binding force with Fe ions on the metal surface regardless of its shape. There are more broad application prospects for SAMs, since a SAM can be used as a transition layer for further modification.

Heteroatoms, such as N and O, have remarkable electronegativity, and, therefore, they play important roles in molecular self-assembly and corrosion inhibition[11-15]. Among them, pyridine and furan are widely used. First, these two reagents are excellent solvents that can penetrate the metal surface and react with Fe ions in the rust layer. Second, the rust layer is tolerant towards the dosage of the reagents because pyridine and furan can be used as corrosion inhibitors in the coating[16-19]. Finally, these two reagents have a strong negative electrical resistance that provides a powerful electron-donating ability that can be matched with an Fe ion in the rust layer. However, there are no available reports regarding pyridine and furan being used as rust converters. In this paper, pyridine and furan that contain N and O atoms were selected for pre-treating a rust layer on the mild surface, and their effects on the performance of a rust coating were evaluated.

## 2. EXPERIMENTAL

### 2.1. Materials

Commercially available A3 ordinary carbon structural steel was used as a substrate. Pyridine (99.5%) and furan (99.5%) were obtained from the Aladdin Company. A dispersant (BYK-161) and an anti-settling agent (BYK-410) were purchased from BYK Additives and Instruments. A defoamer (Dow Corning 1430) was provided by the Dow Corning Industrial Corporation. The rust coating was produced in a lab, and the mixing procedure is briefly introduced as follows. First, 30 g of epoxy resin and 5 g of polyvinyl butyral were dissolved in 20 g of butyl acetate and 10 g of ethanol to produce the main film-forming material. Then, 0.5 g of a dispersant, 0.5 g of a defoamer and 1 g of an anti-settling agent were added to that solution. A functional filler mainly includes 5 g of talc powder and 3 g of iron oxide red pigments. Diethylenetriamine was added as the curing agent. The chemical reagents were all analytical reagent grade and were used without any further treatment.

### 2.2. Methods

A3 steel pieces with dimensions of 15 mm × 15 mm × 5 mm were burnished using 400#, 800# and 1200# sandpaper, cleaned with acetone and ethanol in an ultrasonic cleaning machine, and then dried in air. The samples were sprayed with a 3.5% NaCl solution and dried at room temperature in air. The spray-drying procedure was repeated 4 times in one day, and the spacing interval between the two

experiments was 3 hours. The test was conducted for 14 days. Using this approach, a rust layer was prepared.

Solutions of pyridine (99.5%) and furan (99.5%) were prepared separately at concentrations of 5 mol/L, and alcohol was used as the solvent. Then, the solutions were evenly dropped onto the rusty surface separately using a dropper. The specimens were transferred into a box covered with cling film, and the specimens were stored at room temperature for a week to complete the pretreatment. Finally, when the sample was completely dry, the metal surface was painted with a rust coating.

### 2.3. Testing and characterization

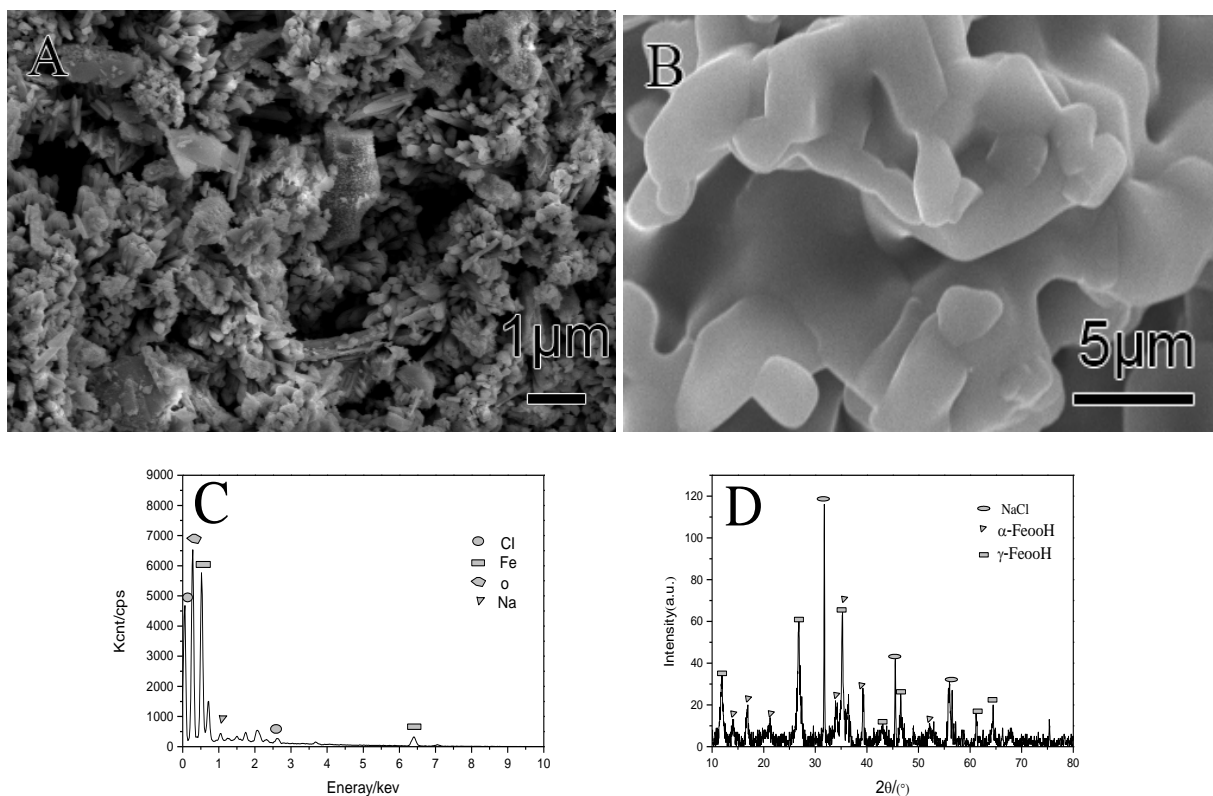
Scanning electron microscopy (SEM) and energy dispersive spectrometry (EDS) studies were carried out using a JSM-6480 scanning electron microscope operating at 15 keV. The coating microtopography and elemental ratio of the product were measured. An X-ray diffraction (XRD-6000) instrument, produced by Shimadzu of Japan, was used to characterize the phases of the sample with Cu-K $\alpha$  radiation. During XRD, the scan speed was 5°/min, and the range was 10°~80°.

Electrochemical tests were conducted using a Solartron 2350 electrochemical interface and a Solartron 1260 impedance/gain-phase analyser. A standard three-electrode configuration consisting of the sample as a working electrode, a counter electrode (CE) and a saturated calomel electrode (SCE) was used to determine polarization behaviours. A saline (3.5% wt. NaCl) solution was used as the corrosive electrolyte. For each sample, the open circuit potential was first measured for a period of half an hour. Then, the impedance was measured and plotted via Zplot from the Windows electrochemical impedance software at the sample's respective corrosion potential. A 10 mV vs SCE AC voltage was used as the imposed signal. The polarization curve was measured in the range of -1.25 V–0.75 V using a constant scan rate of 2 mV/s. To observe the microstructure and elemental distribution of the coating before and after immersion, a saline (3.5% wt. NaCl) solution was used as corrosive medium for the coating immersion. In addition, part of the coating was pulled off using a cutter knife and tweezers to observe the bottom of the coating.

## 3. RESULTS AND DISCUSSION

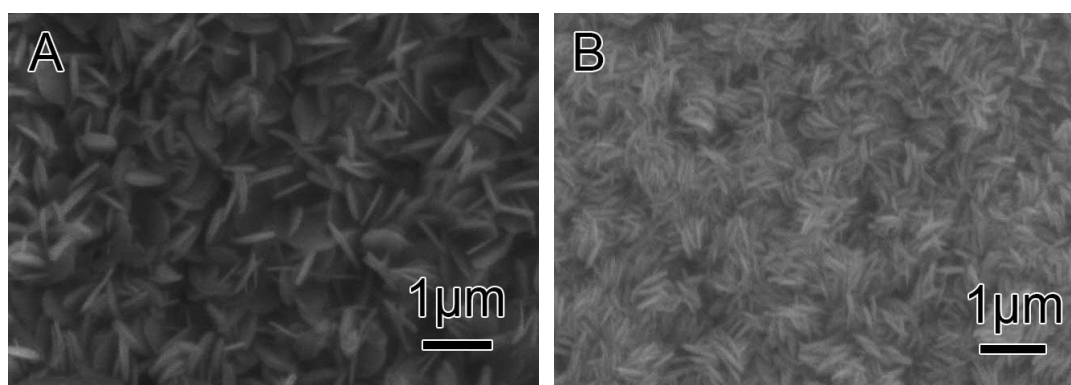
### 3.1 Characterization of the rust layer

Fig. 1 shows the morphology, elemental and phase composition results of the rust layer on the A3 steel specimen. As seen from Fig. 1 A and B, the rust layer is loosely attached on the steel surface, is porous, could not protect the sample and could even induce more serious corrosion. Fig. 1 C shows the layer that consists of sodium, chlorine, iron and oxygen. XRD analysis (Fig. 1 D) reveals that the main components of the rust layer on the A3 specimen are NaCl,  $\alpha$ -FeOOH and  $\gamma$ -FeOOH[20]. The existence of NaCl is due to the spray process used to produce the rust layer.



**Figure 1.** Morphology, elemental and phase composition of the rust layer on the A3 steel specimen.

### 3.2. Morphologies of the rust layer treated by functional organic molecules



**Figure 2.** Observation of the micromorphology of coordination and assembly of the rust steel with pyridine treatment (A) and furan treatment (B).

Fig. 2 shows the morphologies of rust surfaces treated by pyridine (Fig. 2 A) and furan (Fig. 2 B). It can be seen that after the pyridine and furan treatment, the surfaces become more compact and smooth compared to those of the untreated sample. In addition, the rust layer treated with pyridine and furan can distribute evenly on the metal surface, and the surface is more smooth and compact. This is mainly because the two chemicals are remarkable rust converters that can dissolve the rust and make the surface smoother. In addition, phosphoric and tannic acids were chosen as rust converters in some

studies [21-23]. In these studies, the researchers confirmed that the samples with a rust converter are more homogeneous compared with the not-converted ones. A homogeneous converted rust layer was also obtained after the treatment. However, the potential damage of these corrosive reagents on the steel substrate is still a concern.

### 3.3. Corrosion resistance of the treated rust layer

#### 3.3.1 Polarization curves

To determine the corrosion resistance of the surface treated by pyridine and furan, polarization curves and impedance spectra of the samples were determined. Fig. 3 shows the polarization curve of the samples, while the corresponding corrosion electrochemical parameters are shown in Table 1, where  $E_{corr}$ ,  $I_{corr}$  and  $V_{corr}$  represent the corrosion potential, corrosion current and corrosion rate, respectively.

One can observe that the polarization curves of the specimens with pyridine or furan treatment move towards the positive side, as well as the stable potential, which indicates that these two molecular modified films retard anodic polarization and increase anodic polarization in electrochemical corrosion.

It can be seen from Table 1 that the corrosion current and corrosion rate of the metal surfaces treated by pyridine or furan are smaller than of the blank sample. The corrosion resistance of the surface with pyridine and furan treatment is higher than that of the untreated sample. Most of the well-known corrosion inhibitors are organic compounds that contain heteroatoms such as nitrogen, sulphur, phosphorus, and oxygen atoms[24-26]. However, there are some differences among heterocyclic compounds with different elements regarding the reduction of corrosion rate. The corrosion current and corrosion rate of the metal surface treated by pyridine and furan clearly decreased. The heterocyclic compound with the N and O atoms has a stronger ability to supply electrons. This is why the heterocyclic compound with the N and O atoms easily combines with Fe.

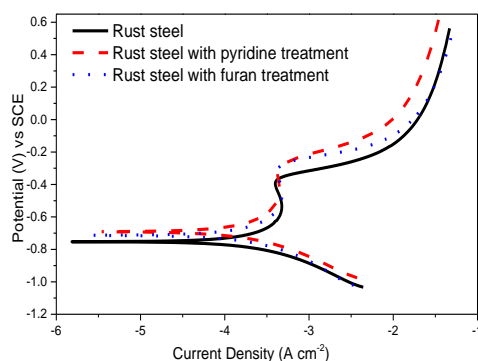


**Figure 3.** Polarization curves of rust steel without treatment (A) or with pyridine treatment (B), furan treatment (C).

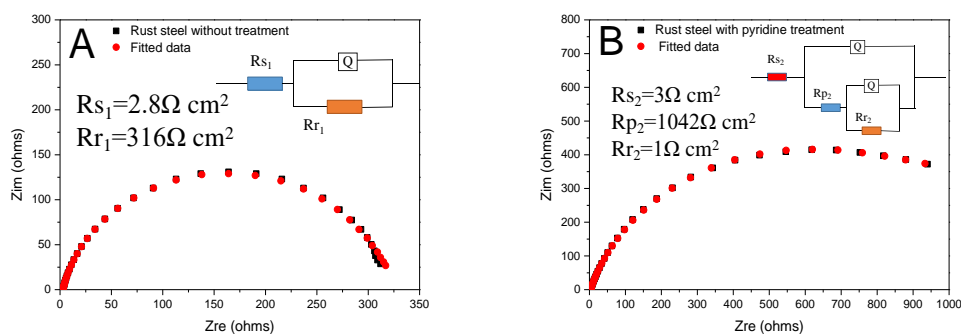
**Table 1.** Corrosion parameters of the rust layer without treatment or with pyridine treatment or furan treatment.

Sample	$E_{corr}/V$	$I_{corr}/mA$	$V_{corr}/(mm/a)$
Rust steel	-0.78	0.23	2.69
Rust steel with pyridine treatment	-0.70	0.14	1.24
Rust steel with furan treatment	-0.72	0.15	1.76

### 3.3.2 Analysis of electrochemical impedance spectroscopy data

The fitted data and the equivalent circuits are shown in this paper. The Nyquist diagrams and representative diagrams of using the equivalent circuits to fit the experimental data are shown in Fig. 4. The solution resistance and polarization resistance of the coating are also shown. The  $R_s$ ,  $R_p$ ,  $R_r$  are used to represent solution resistance, SAM resistance and rust resistance, respectively, while the inductance is represented by  $Q$ . It can be seen from Fig. 4 that  $R_{r1}$  of rust on the surface without treatment is  $316 \Omega \text{ cm}^2$ . The rust resistance with pyridine and furan treatment decreased to  $1 \Omega \text{ cm}^2$  and  $1.6 \Omega \text{ cm}^2$ . This is because the upper part of rust has reacted with functional molecules after the pyridine and furan treatment.  $R_{p2}$  is  $1042 \Omega \text{ cm}^2$ , which represents the pyridine-treated layer resistance, while the furan layer resistance ( $R_{p3}$ ) is  $747.5 \Omega \text{ cm}^2$ . The SAMs of pyridine and furan can improve the protection of metal surface. Furthermore, the protective effect of pyridine is the best.

The main reason that pyridine and furan show differences in improving the corrosion resistance of the metal layers is due to their structures. Pyridine can form a complex compound with the ferric ion. Although the outermost layer of the N atom is saturated, there is a pair of unshared electrons[15]. This is why it is able to supply electrons. For furan, the O atoms in the heterocycle carry two pairs of lone-pair electrons[27]. One pair of them conjugates with two nearby C=C groups, forming a  $\pi$  bond, whereas another pair of electrons is in the outermost layer of the heterocycle. Thus, it can also supply electrons and react with metal ions to form a coordination compound.



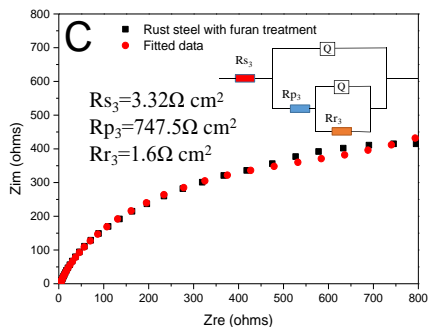


**Figure 4.** Nyquist diagrams and diagrams of using the equivalent circuits to fit the experimental data of rust steel without treatment (A) or with pyridine treatment (B) or furan treatment (C).

3.4. Corrosion resistance of the composite coating on metal surface

3.4.1. Adhesion strength

The adhesion of EP-PVB coating to bare steel, rust-covered steel, and pyridine- and furan-treated specimens was tested according to ISO 2409[28]. It can be seen from Fig. 5. That after rust formation, there is considerable peeling on the specimens, while the EP-PVB coatings on the surface with pyridine and furan treatment were still complete, which is the same as the EP-PVB coating without rust. The pyridine and furan pretreatment achieves good adhesion that can be rated as 0 according to the ISO 2409 standard[28], and this result is comparable with the best results from another study [29]. This result shows that pyridine and furan can improve the adhesion of EP-PVB coatings to rust-covered mild steel.

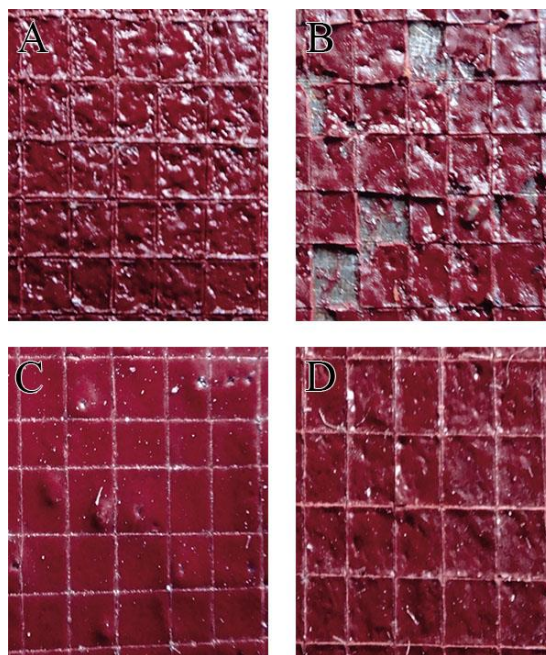


**Figure 5.** Adhesion test results for the coatings: coating without rust (A), rust/coating (B), pyridine/coating (C), and furan/coating (D).

3.4.2. Polarization curves of the EP-PVB coatings

Fig. 6 shows the polarization curves of rust coatings that were painted onto the surface with pyridine and furan pretreatment, separately, or without treatment. The electrochemical corrosion parameters are shown in Table 2. The corrosion potential of pyridine/coating and furan/coating move towards the positive side, while the corrosion currents decreased significantly. In addition, both pyridine/coating and furan/coating retard the processes occurring at the cathode and anode separately.

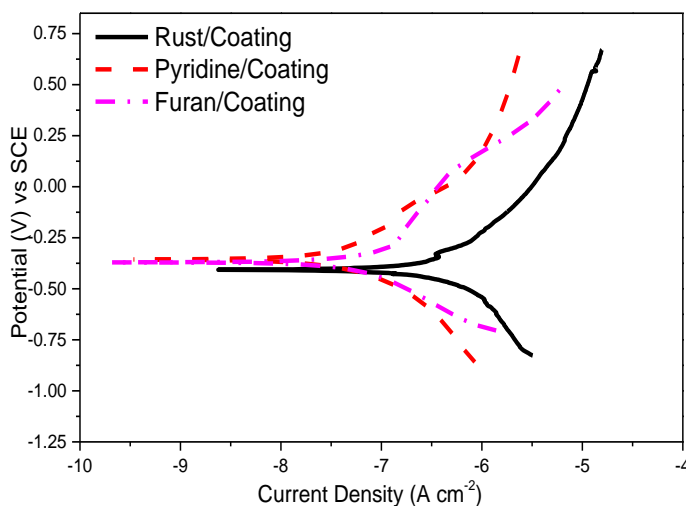


**Figure 6.** Polarization curves of EP-PVB-coated specimens without or or with pyridine treatment or furan treatment.

To explain the function of the heterocyclic compounds more clearly, there is a careful description of the data in Table 2. It is clear that the corrosion current and corrosion rate of rust coatings painted onto the surface with pyridine and furan treatment separately are smaller than those of the sample without a pretreatment. The parameters of the polarization of pyridine/coating and furan/coating are similar. Chemically, the N and O atoms are more likely to coordinate with Fe ions. Furthermore, physically, the holes in the rust layer were repaired via physical filling due to the chemical combination. The corrosion current of coatings on surface with pyridine or furan treatment are similar with the former research[4].

**Table 2.** Corrosion parameters of the EP-PVB-coated specimens without treatment or with pyridine treatment or furan treatment.

Type	$E_{corr} / V$	$I_{corr} / \mu A$	$V_{corr} / (\mu m/a)$
Rust/coating	-0.41	83.48	56.59
Pyridine/coating	-0.39	0.23	0.15
Furan/coating	-0.39	0.30	0.20

3.4.3. Electrochemical impedance spectroscopy

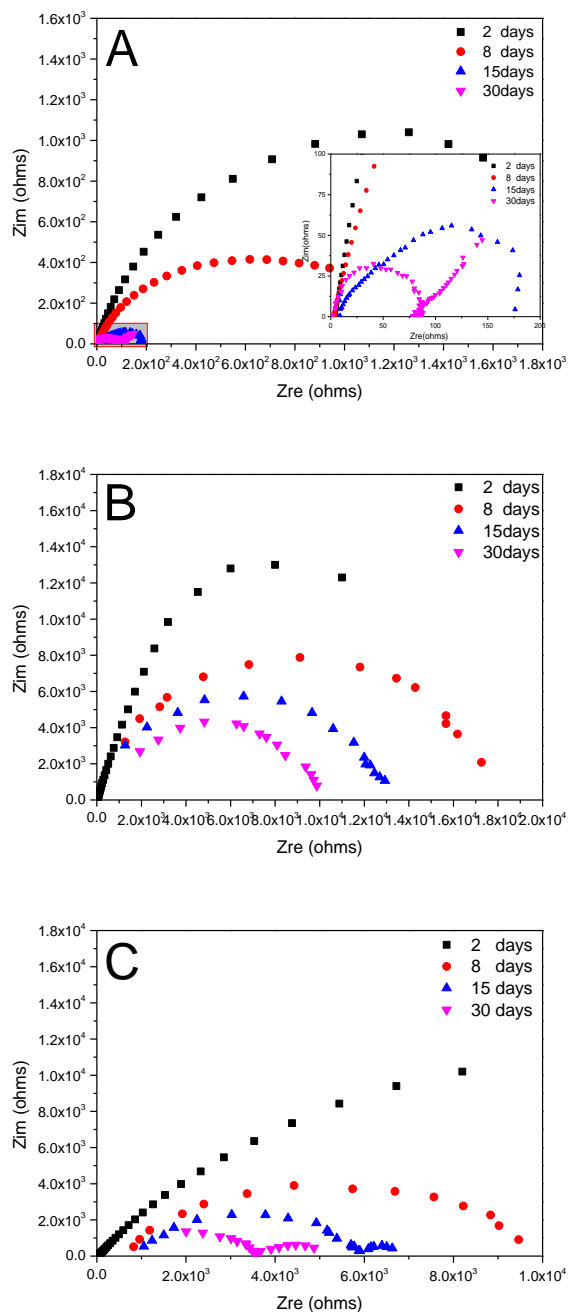


**Figure 7.** Nyquist diagrams of the EP-PVB coating on the surface without treatment (A) or with pyridine treatment (B) or furan treatment (C)

Fig. 7 shows the electrochemical impedance spectroscopy of the samples. The impedance of the coatings on the surface pretreated by pyridine and furan individually is higher than that of the surface without pretreatment, even after 30 days of immersion in a NaCl solution. Specifically, after 2 days, the impedance was still large, and the protective effect of rust coating was perfect, which means that the corrosion medium was well insulated from the coating. Then, the impedance decreased slightly

when the coating was immersed for 8 days, which means that although aggressive medium spread into the rust coating, it had not arrived at the metal surface. Finally, with the extension of soaking time, the protective effect of rust coating further decreased, which means that the coating will gradually fail.

It is worth noting that after being soaked for 15 and 30 days, the pyridine/coating sample still presented a single capacitive impedance arc, which indicated the initial stage of immersion, although the protective effect of the coating had clearly decreased. On the other hand, there were two capacitive arcs when the furan/coating was soaked for 15 days and 30 days, which indicated that immersion had entered the late stage. At this moment, aggressive medium had penetrated the coating, and the electrochemical reaction had started. Generally, the protective effect of the coating decreases with the immersion time as a smaller number of H<sub>2</sub>O, O<sub>2</sub> and Cl<sup>-</sup> molecules penetrated into the coatings [30].

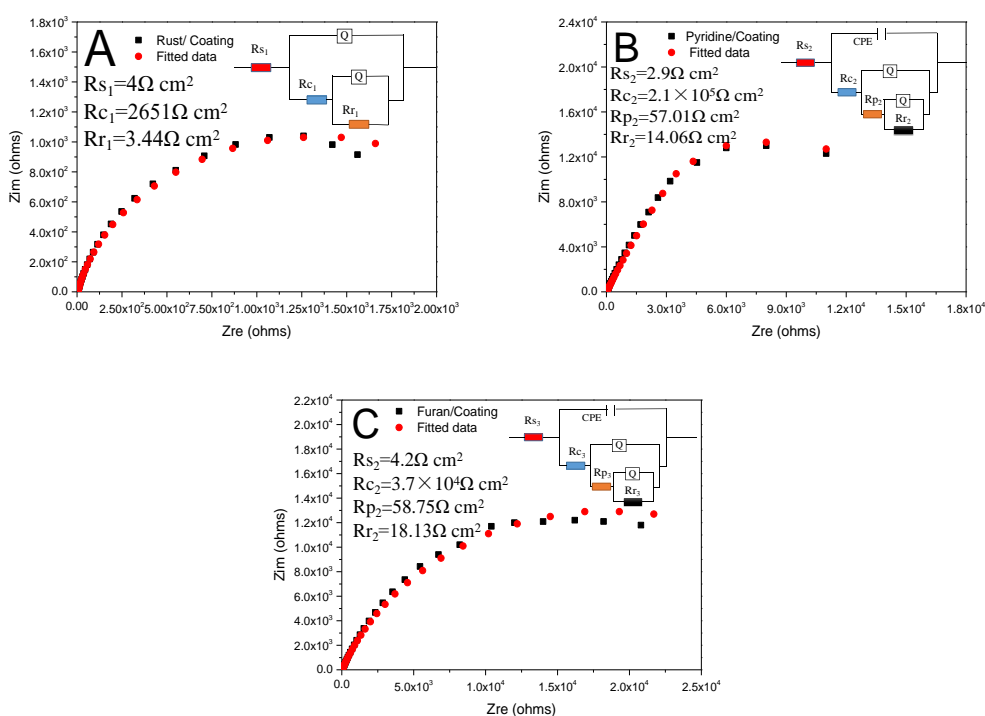


**Figure 8.** Representative diagrams of the equivalent circuits to fit the experimental data of rust steel without treatment (A) or with pyridine treatment (B) or furan treatment (C) after 2 days of immersion

Representative diagrams of the equivalent circuits to fit the experimental data of the EP-PVB-coated rust steel are shown in Fig. 8. In previous studies [31,32], the reaction product of rust converter with rust is a film of ferrite. So the SAM resistance still exists. *Rs*, *Rp*, and *Rr* represent the solution resistance, SAM resistance and rust resistance, respectively. The coating resistance is represented by *Rc*, and the constant phase element is represented by CPE. According to the abovementioned diagrams, the stable value of *Rc*<sub>1</sub> increased from 2651 Ω cm<sup>2</sup> to 2.1×10<sup>5</sup> Ω cm<sup>2</sup> (*Rc*<sub>2</sub>) and 3.7×10<sup>4</sup> Ω cm<sup>2</sup> (*Rc*<sub>3</sub>) with pyridine and furan treatment, respectively. Clearly, the diagrams reveal that the protection of the coating on the surface with pyridine and furan treatment was much better than that without the treatment when the coating was soaked in a 3.5% NaCl solution for 2 days. Furthermore, the protection of the coating on the surface with pyridine was the best compared with the other two sample.

3.4.4. Microstructure and elemental distribution of the coating before and after immersion

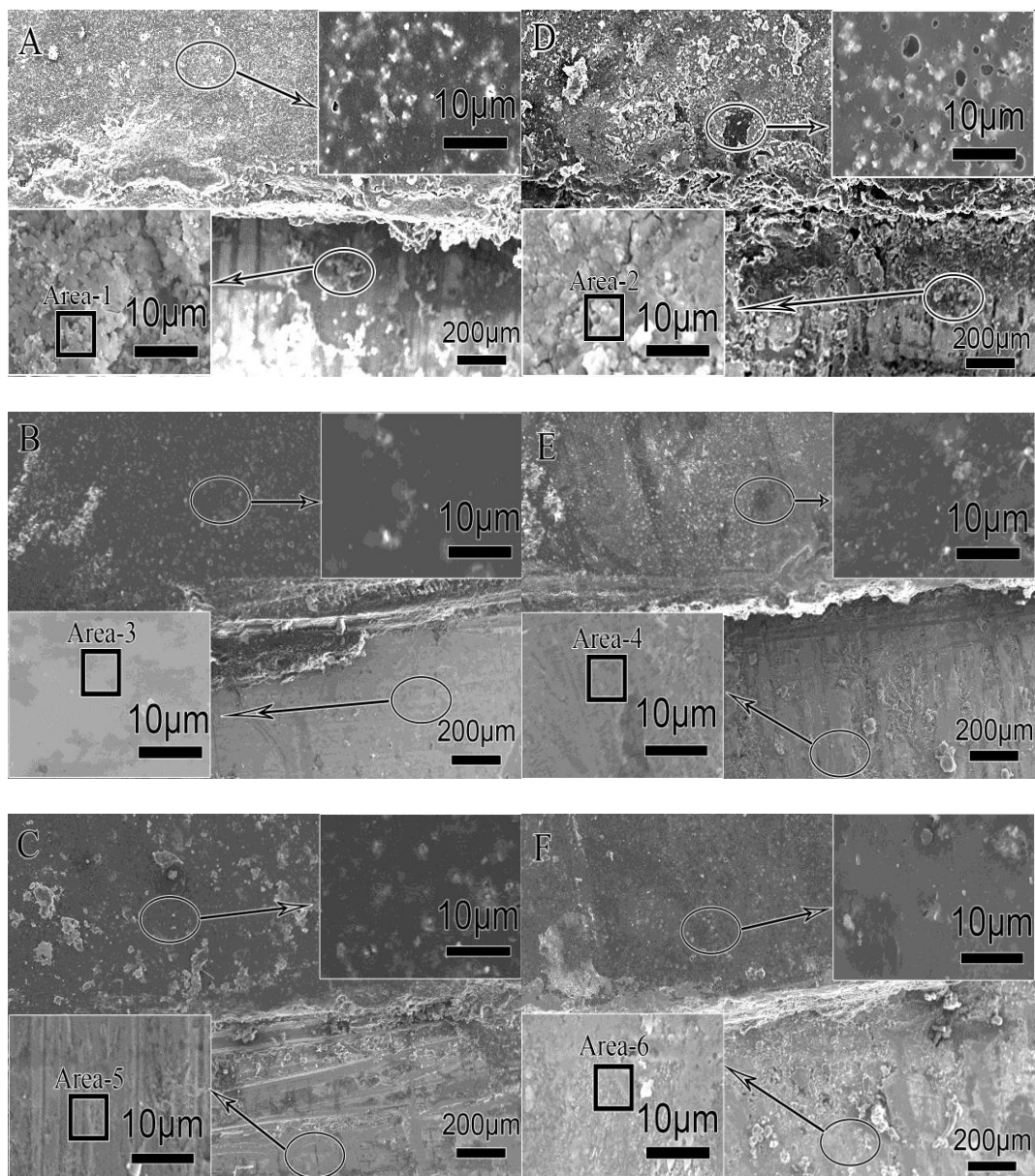


**Figure 9.** Microstructure and elemental distribution of the coating before and after immersion: A. coating without treatment, B. coating with pyridine treatment, and C. coating with furan treatment. D, E, F are after the immersion of A, B, C.

Fig. 9 A, B and C show the surface morphologies of the coatings without pretreatment and with pyridine and furan treatment before the corrosion test. Fig. 9 D, E and F show the micro-morphology of coatings after immersion in NaCl solution for 30 days. The upper part of the topography is the morphology of the coating, while the lower part is the microscopic appearance of the substrate after peeling off the coating. The EDS results of the circled areas are listed in Table 3.

It can be seen from Fig. 9 A that the coating surface of the untreated sample is rough and porous. In addition, there are many rust particles that remain on the substrate surface when the coating was peeled off. The EDS of area 1 shows that the content of O is higher than that of Fe. The holes in

the coating in Fig. 9 D are clearly more abundant than before corrosion, as well as the amount of rust. In addition, EDS indicates that there are many more O atoms than before.

**Table 3.** EDS analysis of the metal surface without treatment or with pyridine treatment or furan treatment before and after immersion.

Area	Atomic percentage %					Total
	O	Fe	N	Na	Cl	
Area-1	51.72	37.57	-	6.69	4.02	100
Area-2	61.42	36.27	-	2.17	0.14	100
Area-3	14.83	31.8	53.37	-	-	100
Area-4	16.81	68.86	13.52	0.61	0.20	100
Area-5	18.26	78.98	-	2.60	0.16	100
Area-6	17.15	82.85	-	-	-	100

The untreated rust layer on the bottom of the coating cannot help prevent corrosion. Fig. 9 B shows that the coating on the surface with pyridine pretreatment is compact. The substrate surface is very smooth, and there is no rust residue. The EDS of area 3 shows that the substrate surface contains N and Fe elements. This shows that pyridine was attached to the metal surface, and the surface rust layer was completely converted into harmless filler in the EP-PVB coating. Fig. 9 E shows that the coating surface after corrosion is still dense, and the EDS analysis in area 4 shows that there is a small amount of rust, which means that the protective properties of the coating are excellent. Finally, as seen in Fig. 9 C, the coating on the surface with furan treatment was as dense as that with pyridine treatment. There was no large amount of rust remaining on the surface after peeling of the coating because the majority of rust was combined into the coating as a filler. Whereas in the case of the samples without pretreatment, only the loose layer of rust participated in the curing of EP-PVB, and the bottom layer that was left as the coating was removed. The EDS results in area 5 also confirm this conclusion. There are no clear defects in the coating with furan treatment after corrosion (Fig. 9 F). The EDS in area 6 shows that the area only contains O and Fe atoms, and the content of O element is less than that of Fe element. All abovementioned results show that corrosion resistance of the coating on the surface with pyridine and furan pretreatment was significantly improved compared with the untreated samples. The rust layer combined into rust coatings if pretreatment was conducted and was converted into harmless fillers. This phenomenon increased the adhesion strength of the coating as well as its corrosion resistance. These results indicate that EP-PVB coating could form covalent bond [33]. Moreover, pyridine pretreatment is more effective according to our results. In other's rust coating

system[4], the surface is more uniform than the surface without phosphate treatment after peeling off the coating.

#### 4. CONCLUSIONS

Pyridine and furan can coordinate with rust on mild steel spontaneously by forming self-assembled monolayers (SAMs) that can improve the corrosion resistance of the rust-covered metal. The pretreatment with pyridine and furan can also transform the porous rust on steel into dense filler for further coatings. Thus, the corrosion resistance and adhesion of rust coating on steel can be clearly improved.

#### ACKNOWLEDGEMENTS

We gratefully acknowledge the financial support from the Natural Science Foundation of the Jiangsu Province (BK20160566), China Postdoctoral Science Foundation (2016M601754), Jiangsu Planned Projects for Postdoctoral Research Funds (1421601085B), and Jiangsu Provincial Department of Education Fund (15KJB430009).

#### References

1. J. M. Lehn, *Sci.*, 295(5564) (2002) 2400-2403.
2. G. S. Papaefstathiou, L. R. Coordin, *Chem. Rev.*, 246(1) (2003) 169-184.
3. J. M. Lehn, *Polym. Int.*, 51(10) (2002) 825-839.
4. J. H. Ding, H. R. Zhao, L. Gu, S. P. Su, H. B. Yu, *Int. J. electrochem. sci.*, 11 (2016) 7066-7075.
5. U. Harm, R. Burgler, W. Furbeth, K.M. Mangold, K. Jüttner, *Macromol. Sym.*, 187 (2002) 65-75.
6. S. Tadashi, A. Kunitsugu, *Corros. Sci.*, 50(2) (2008) 596-604.
7. A. Kunitsugu, S. Tadashi, *Corros. Sci.*, 53(12) (2011) 4152-4158.
8. A. Paszternák, I. Felhősi, Z. Pászti, E. Kuzmann, A. Vértes, E. Kálmán, L. Nyikos, *Electrochim. Acta*, 55(3) (2010) 804-812.
9. F. E. Heikal, A. S. Fouda, M. S. Radwan, *Mater. Chem. Phy.*, 125 (1) (2011) 26-36.
10. M. Volmer-Uebing, B. Reynders, M. Stratmann. *Mater. Corros.*, 42 (1) (1991) 19-34.
11. S. Hong, W. Chen, H. Q. Luo, N. B. Li, *Corros. Sci.*, 57 (2012) 270-278.
12. A. Kunitsugu, S. Tadashi, *Corros. Sci.*, 46 (2) (2004) 313-328.
13. K. Aramaki, T. Shimura, *Corros. Sci.*, 52 (9) (2010) 2766-2772.
14. A. Paszternák, I. Felhősi, Z. Pászti, L. Nyikos, *Electrochim. Acta*, 55 (2010) 804-812.
15. F. EI-Taib. Heikal, A. S. Foude, M. S. Redwan, *Mater. Chem. Phy.*, 125 (2011) 26-36.
16. K. R. Ansari, M. A. Quraishi, A. Singh, *Meas.*, 76 (2015) 136-147.
17. M. A. Bedair, *J. Mol. Liq.*, 219 (2016) 128-141.
18. B. Xu, Y. Ji, X. Q. Zhang, X. D. Jin, W. Z. Yang, Y. Z. Chen, *J. Taiwan Inst. Chem. E.*, 000 (2015) 1-10.
19. Y. Ji, B. Xu, W. N. Gong, X. Q. Zhang, X. D. Jin, W. B. Ning, Y. Meng, W. D. Yang, Y. Z. Chen, *J. Taiwan Inst. Chem. E.*, 000 (2016) 1-12.
20. S. Nasrazadani, *Corros. Sci.*, 39 (1997) 1845.
21. L.M. Ocampo, I.C.P. Margarit, O.R. Mattos, S.I. Cordoba-de-Torresi, F.L. Fragata, *Corros. Sci.*, 46 (2004) 1815.
22. A. A. Rahim, M. J. Kassim, E. Rocca, J. Steinmetz, *Corros. Eng. Sci. and Technol.*, 46 (4) (2011) 425-43.
23. Y. Li, Y. T. Ma, B. Zhang, B. Lei, Y. Li, *Acta. Metall. Sin-Engl.*

- 27(6) (2014) 1105-1113.
24. M.A. Deyab, *Corros. Sci.*, 49 (2007) 2315.
  25. A.M. Alsabagh, M.A. Migahed, H. S. Awad, *Corros. Sci.*, 48 (2006) 813.
  26. S. Ghareba, S. Omanovic, *Corros. Sci.*, 52 (2010) 2104-2113.
  27. K. Aramaki, T. Shimura, *Corros. Sci.*, 46 (2004) 213-328.
  28. ISO 2409, ISO, Geneva (2013) pp. 1-18.
  29. S. Martinez, B. Miksic, I. Rogan, A. Ivakovic, *the annual event of the European Federation of Corrosion*. 9 (2016) 11-15.
  30. H. Wei, D. Ding, S. Wei, and Z. Guo, *J.Mater. Chem. A*, 1 (2013) 10805.
  31. D. Vacchini, *Anti-Corros.*, 9 (1985) 9.
  32. W. Meisel, H.J. Guttmann and P. Gutlich, *Corros. Sci.*, 23 (1983) 1373.
  33. L. Gu, J. Ding, S. Liu, and H. Yu, *Chinese J. Chem. Phys.*, 29 (2015) 271.

© 2017 The Authors. Published by ESG ([www.electrochemsci.org](http://www.electrochemsci.org)). This article is an open access article distributed under the terms and conditions of the Creative Commons Attribution license (<http://creativecommons.org/licenses/by/4.0/>).